Synthetic and Systems Biotechnology 9 (2024) 187–195

Contents lists available at ScienceDirect

Synthetic and Systems Biotechnology

journal homepage: www.keaipublishing.com/en/journals/synthetic-and-systems-biotechnology

Original Research Article

Efficient conversion of aromatic and phenylpropanoid alcohols to acids by the cascade biocatalysis of alcohol and aldehyde dehydrogenases

Zetian Qiu [a,b,1], Xiaohui Liu [a,1], Jie Yu [c], Yushuo Zhao [a], Guang-Rong Zhao [b], Shengying Li [a], Kun Liu [a,**], Lei Du [a,***], Li Ma [a,*]

[a] State Key Laboratory of Microbial Technology, Shandong University, Qingdao, Shandong, 266237, China
[b] Frontier Science Center for Synthetic Biology and Key Laboratory of Systems Bioengineering (Ministry of Education), School of Chemical Engineering and Technology, Tianjin University, Yaguan Road 135, Jinnan District, Tianjin, 300350, China
[c] School of Health Management, Hengxing University, Qingdao, Shandong, 266100, China

ARTICLE INFO

Keywords:
Benzyl acids
Phenylpropanoid acids
Alcohol dehydrogenases
Aldehyde dehydrogenases
Whole-cell catalysis

ABSTRACT

Benzyl and phenylpropanoid acids are widely used in organic synthesis of fine chemicals, such as pharmaceuticals and condiments. However, biocatalysis of these acids has received less attention than chemical synthesis. One of the main challenges for biological production is the limited availability of alcohol dehydrogenases and aldehyde dehydrogenases. Environmental microorganisms are potential sources of these enzymes. In this study, 129 alcohol dehydrogenases and 42 aldehyde dehydrogenases from *Corynebacterium glutamicum*, *Pseudomonas aeruginosa*, and *Bacillus subtilis* were identified and explored with various benzyl and phenylpropanoid alcohol and aldehyde substrates, among which four alcohol dehydrogenases and four aldehyde dehydrogenases with broad substrate specificity and high catalytic activity were obtained. Moreover, a cascade whole-cell catalytic system including ADH-90, ALDH-40, and the NAD(P)H oxidase LreNox was established, which showed high efficiency in converting cinnamyl alcohol and *p*-methylbenzyl alcohol into the respective carboxylic acids. Remarkably, this biocatalytic system can be easily scaled up to gram-level production, facilitating preparation purposes.

1. Introduction

Benzyl compounds and phenylpropanoids serve as crucial intermediates in the production of fine chemicals and active metabolites that have broad applications and high industrial value [1,2]. Their aldehydes, such as vanillin, benzaldehyde, and cinnamaldehyde, are prized for their aromatic properties and account for the fragrance industries, which have an estimated global market value of approximately $ 1 billion [3]. Their carboxylic acids, including salicylic acid, ferulic acid, gallic acid, and *p*-coumaric acid, are commercially important compounds that have diverse uses in the food, pharmaceutical, cosmetic, and chemical industries [4]. Derivatives of benzyl and phenylpropanoid acids, such as flavonoids and resveratrol, are noteworthy for their remarkable health benefits and medicinal activity [5]. The market share of flavonoids is projected to reach $ 3.5 billion by 2025 [6], while resveratrol is anticipated to attain a market share of $ 99.4 million [7].

Carbonyl compounds, including benzyl and phenylpropanoid aldehydes and carboxylic acids, can be produced by the oxidation of alcohols, and the catalytic synthesis process has attracted considerable attention from organic chemistry chemists and biochemists. Selective oxidation of benzyl alcohols and phenylpropanoid alcohols can afford their benzyl and phenylpropanoid aldehyde analogues, which can be further oxidized to yield the corresponding benzyl and phenylpropanoid carboxylic acids [8,9]. Direct selective oxidation of alcohols and aldehydes in a chemical process is well-established [10,11], such as chromium and manganese oxide catalysis [12,13], Dess-Martin oxidation [14], Swern oxidation [15], and noble metal catalyst systems [16].

Peer review under responsibility of KeAi Communications Co., Ltd.
* Corresponding author.
** Corresponding author.
*** Corresponding author.
E-mail addresses: liuk@sdu.edu.cn (K. Liu), lei.du@sdu.edu.cn (L. Du), maliqd@sdu.edu.cn (L. Ma).
[1] These authors contributed equally.

https://doi.org/10.1016/j.synbio.2024.01.008
Received 15 September 2023; Received in revised form 24 December 2023; Accepted 19 January 2024
Available online 5 February 2024

However, there are fewer reports on biocatalysis, and achieving high-efficient and green biocatalysis remains a significant challenge.

Alcohol dehydrogenase (ADH) is a member of the dehydrogenase family found in various organisms. It catalyzes the oxidation of primary and secondary alcohols into the corresponding aldehydes or ketones [17]. Aldehyde dehydrogenase (ALDH) belongs to the nicotinamide adenine dinucleotide (phosphate) (NAD(P))-dependent enzyme family. It oxidizes a wide range of aliphatic and aromatic aldehydes, both endogenous and exogenous, to form the corresponding carboxylic acids [18]. The biocatalytic potential of ADH and ALDH is particularly attractive for the selective cascade oxidation of benzyl alcohols and phenylpropanoid alcohols to produce corresponding carboxylic acids [19]. Environmental microorganisms, such as *Corynebacterium* [20], *Pseudomonas* [21], and *Bacillus* [22], exhibit remarkable abilities to degrade and oxidize phenolic compounds through catalysis of alcohols, aldehydes and acids, highlighting their potential as candidate dehydrogenases [23–28]. Exploring potential dehydrogenases in environmental microorganisms opens up opportunities for the efficient biocatalysis of these compounds [29].

In this study, the genomes of representative environmental microorganisms *C. glutamicum* ATCC 13032, *P. aeruginosa* PAO1, and *B. subtilis* subsp. 168 were analyzed, and 129 alcohol dehydrogenases and 42 aldehyde dehydrogenases were identified. Representative benzyl and phenylpropanoid alcohols and aldehydes were tested as substrates, and 4 ADHs and 4 ALDHs with broad substrate specificity and high catalytic activity were obtained. Furthermore, a whole-cell cascade biocatalytic system including the optimal dehydrogenases ADH-90 and ALDH-40, as well as the NAD(P)H oxidase LreNox, which was introduced to regenerate NAD^+ and $NADP^+$, was established. Efficient production of benzyl and phenylpropanoid acids was achieved and successfully scaled up to the gram level. Our results provide new insights into the design and construction of other biological redox reactions for natural product synthesis.

2. Materials and methods

2.1. Strains, plasmids and culture conditions

The strains and plasmids used in this study are listed in Table S1 and Table S2. *E. coli* DH5α served as the host for gene cloning and plasmid construction, and was grown on Luria-Bertani (LB) agar plates or LB broth. For protein expression, purification, and biotransformation, *E. coli* BL21 (DE3) was used and grown in LB or Terrific Broth (TB) medium (1.2% tryptone, 2.4% yeast extract, 0.94% K_2HPO_3, 0.22% KH_2PO_3, 4% glycerol). Unless otherwise stated, all *E. coli* strains were incubated at 37 °C, with appropriate antibiotics added to the broth as needed.

2.2. Molecular manipulation, chemicals and reagents

Standard molecular cloning techniques including gene cloning, plasmid transformation, and agarose gel electrophoresis were performed following standard protocols. Primers were listed in Table S2, which were synthesized by Sangon Biotech (Shanghai, China) The primary screened ADHs and ALDHs were amplified from the genome by PCR and cloned between the *Eco*RI and *Nde*I sites of pET30a using restriction enzyme ligation. The LreNox from *Lactobacillus reuteri* was amplified using primers P347 and P348. The pET-28b plasmid and LreNox gene were digested with *Eco*RI (NEB, Frankfurt, Germany) and *Nde*I (NEB, Frankfurt, Germany) at 37 °C for 1 h for linearization, and subsequently constructed into pET28a-LreNOX vector using T4 DNA ligase. The construction method of pETDuet-1-ADH-90-2-ALDH-40 is the same as above. Firstly *ADH*90 was cloned between *Hin*dIII and *Bam*HI of pETDuet-1 to construct pETDuet-1-ADH-90. Then, *ALDH*40 was cloned between *Nde*I and *Xho*I of pETDuet-1-ADH-90 to construct pETDuet-1-ADH-90-2-ALDH-40. The recombinant plasmid was transformed into *E. coli* BL21 (DE3) to generate the recombinant strain. E.Z.N.A.™ Plasmid Miniprep Kit (Omega Biotek, Norcross, GA) was used for plasmid isolation. E.Z.N.A.™ Gel Extraction Kit (Omega Biotek, Norcross, GA) was used for DNA fragment purification. T3 Super PCR Mix (Tsingke Biotechnology, Beijing, China) was used for colony PCR. PrimeSTAR (Takara Bio) or Phanta Max Super-Fidelity DNA polymerase (Vazyme Biotech, Nanjing, China) was used for other conventional PCR amplifications. ClonExpress Ultra One Step Cloning Kit (Vazyme Biotech, Nanjing, China) was used for plasmid construction. All substrates and chemicals were purchased from Shanghai Aladdin Biochemical Technology Co., Ltd., Shanghai Macklin Biochemical Technology Co., Ltd. or Sigma Aldrich (Shanghai) Trading Co., Ltd.

2.3. Protein expression, purification and concentration determination

A single colony of *E. coli* BL21 (DE3) harboring the specific expression plasmid was grown in 5 mL LB broth with 50 μg/mL kanamycin and incubated at 37 °C, 220 rpm, overnight. Then, the overnight culture (500 μL) was inoculated into 500 mL of fresh TB broth containing kanamycin and incubated at 37 °C, 220 rpm. When the cell density reached an OD_{600} of 0.6–0.8, IPTG was added to a final concentration of 0.2 mM. The cells were continued to grow at 18 °C for 24 h and then harvested by centrifugation at 6000 g, 4 °C. The cell pellets were stored at −80 °C for later use.

All protein purification procedures were performed at 4 °C. Briefly, the cell pellet was resuspended by vortexing in 50 mL of lysis buffer (50 mM NaH_2PO_4, 300 mM NaCl, 10% glycerol, and 10 mM imidazole, pH 8.0). After sonication (5 s on, 5 s off, 30 min total), the crude cell lysate was centrifuged at 12,000×*g* for 30 min. The supernatant fraction was collected, mixed with 1 mL of Ni-NTA resin (Qiagen, Hilden, Germany), and incubated at 4 °C for 30 min on a gentle rotator. The slurry was then loaded onto an empty column for protein purification. The resin was washed with 100 mL of wash buffer (50 mM NaH_2PO_4, 300 mM NaCl, 10% glycerol, and 20 mM imidazole, pH 8.0) until no protein is detectable in the flow-through by Coomassie Brilliant Blue G250 assay. The target protein bound to Ni-NTA resin was eluted with 10 mL of elution buffer (50 mM NaH_2PO_4, 300 mM NaCl, 10% glycerol and 250 mM imidazole, pH 8.0). The eluate was concentrated at 5000 g for 30–60 min using an Amicon Ultra centrifugal filter (Merck KGaA, Darmstadt, Germany). Next, the protein solution was loaded onto a pre-equilibrated PD-10 column (GE Healthcare, Buckinghamshire, UK) for buffer exchange with 5 mL of desalting buffer (50 mM NaH_2PO_4, 10% glycerol, pH 7.5). Finally, the desalted protein fraction was aliquoted, snap-frozen with liquid nitrogen, and stored at -80 °C. Protein concentrations were determined by the Bradford method using BSA as a standard.

2.4. Preparation of a crude enzyme extract

Sterilized 96-well deep well plates were filled with 300 μL of LB medium containing 50 μg/mL kanamycin. Single colonies were inoculated and grown at 37 °C and 220 rpm for 12 h. Then, 10% of the overnight culture was transferred to a new 96-well deep well plate with 400 μL of TB medium containing 50 μg/mL kanamycin per well. The plate was incubated at 37 °C and 220 rpm for 4 h. After that, IPTG was added to a final concentration of 0.2 mmol/L and the plate was incubated at 20 °C and 220 rpm for 20 h. The cells were harvested by centrifugation at 3700 g for 10 min and resuspended in 200 μL of potassium phosphate buffer (50 mmol/L, pH 7.4) containing 100 mg/L lysozyme, 300 U/mL DNase I and 10% Triton X-100. The plate was centrifuged, and the supernatant was collected as the crude enzyme extract.

2.5. Enzymatic assays and kinetics determination

To screen ADHs and ALDHs initially, the *in vitro* enzymatic reaction

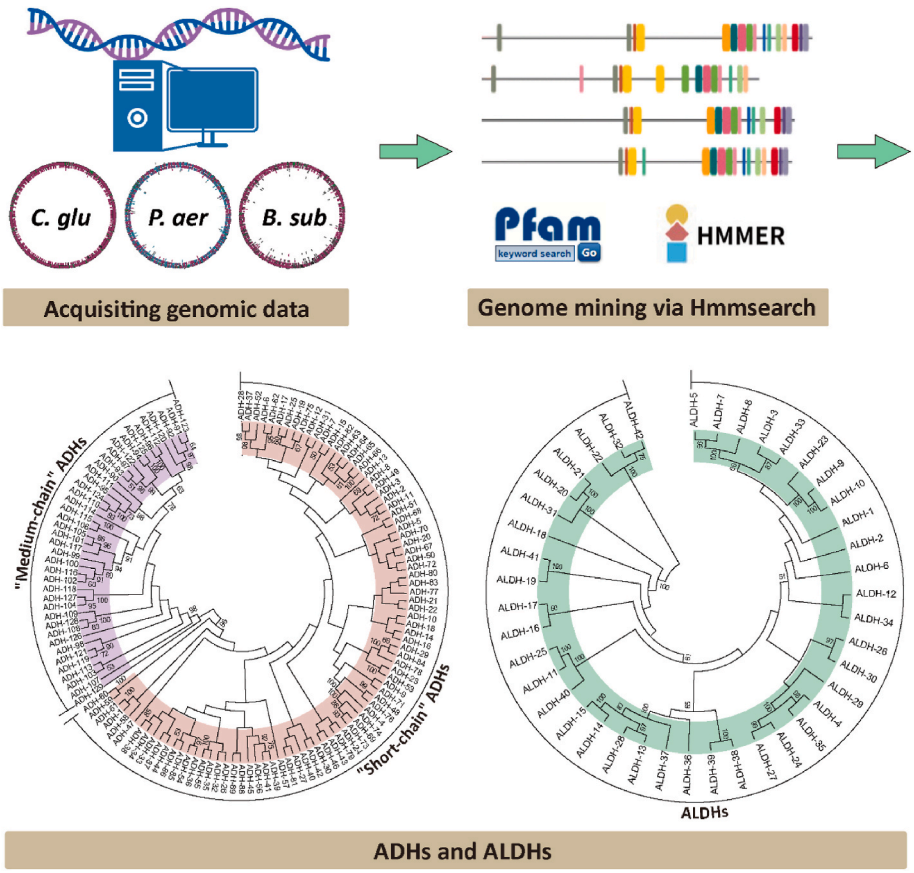

Fig. 1. Genome mining of *P. aeruginosa* PAO1, *C. glutamicum* ATCC 13032, and *B. subtilis* subsp. 168 for ADHs and ALDHs.

system consisted of 1 mM substrate, 1 mM NAD^+, 1 mM $NADP^+$, and 150 μL crude enzyme. To test the substrate promiscuity of pure enzymes, the *in vitro* enzymatic reaction system contained 10 μM ADH or ALDH, 10 μM LreNox, 1 mM substrate, 1 mM NAD^+, and 1 mM $NADP^+$ for 3 h.

To test the thermostability and kinetic parameters, the *in vitro* enzymatic reaction system contained 5 μM ADH-90 or 0.5 μM ALDH-40, 1 mM substrate, and 2 mM NAD^+ at seven temperatures of 0, 25, 30, 35, 40, 45, and 50 °C for 30 min. To test the cofactor preference, the *in vitro* enzymatic reaction system contained 0.5 μM ADH or ALDH, 1 mM substrate, and 2 mM NAD^+ or $NADP^+$ for 10 min. All screening enzymatic assays were performed in 100 μL of 50 mM Tris·HCl buffer (pH 8.0) at 30 °C. The reaction was quenched with two volumes of methanol. The enzyme concentrations of ADH-90 and ALDH-40 in kinetics assays were 5 μM and 0.5 μM, respectively. The triplicated data were fitted to the Michaelis-Menten equation for calculating the k_{cat} and *Km* values of each substrate using Origin 8.5.

2.6. Whole-cell transformation

Recombinant *E. coli* were incubated overnight at 37 °C and 220 rpm. Then, the overnight culture (500 μL) was inoculated into fresh TB broth containing the corresponding antibiotic and incubated at 37 °C and 220 rpm. When the cell density reached an OD_{600} of 0.6–0.8, IPTG was added to a final concentration of 0.2 mM, and the cells were allowed to grow at 18 °C for 24 h. Afterward, cells were harvested by centrifugation at 6000 g and 4 °C, and washed twice with 0.9% NaCl solution. The bacterial cells were resuspended in a solution of $OD_{600} = 27$ for following whole-cell catalysis. A 10 mL volume of the cell suspension was used in a 50 mL Erlenmeyer flask at 30 °C and 220 rpm for the catalytic test. During sampling, 0.5 mL of the transformation solution was mixed with 0.5 mL of methanol and shaken for 1 h, followed by centrifugation at 12,000 rpm for 10 min. The supernatant was then analyzed using HPLC (three parallel experiments were performed).

2.7. Analytical methods

Samples were analyzed on an Agilent 1260 system equipped with a photodiode array detector. Separation was achieved within 15 min using a linear mobile phase gradient on a YMC Triart-C18 column (150 × 4.6 mm, 5 μm). The solvent system consisted of water with 0.1% TFA (solvent A) and acetonitrile (solvent B), and the following linear gradient program was used: 5% buffer B (0–2 min), 5–90% linear gradient of buffer B (2–12 min), 90 to 5% linear gradient of buffer B (12–13 min), and 5% buffer B (13–15 min). The flow rate was set at 1 mL/min, and the injection volume was 10 μL. Full-wavelength scans (210–400 nm) were recorded. Substrate consumption and product formation were quantified by HPLC peak area integration using corresponding authentic compounds as standards.

3. Results and discussions

3.1. Genome mining of environmental microorganisms for alcohol dehydrogenases and aldehyde dehydrogenases

Environmental microorganisms are crucial for ecosystem functioning, as they participate in biogeochemical cycles of various elements, such as carbon, nitrogen, and sulfur [30]. Moreover, they have strong redox capabilities, which enable them to perform functions such as bioremediation, organic matter decomposition, pollutant degradation, and restoration of degraded land [31]. *C. glutamicum*, *P. aeruginosa*, and *B. subtilis*, isolated from sewage and other environments, can efficiently degrade phenol [32,33], formaldehyde [34], *p*-nitrophenol [35], *p*-cresol [36], and diverse polyphenolic compounds [33]. These processes often involve dehydrogenase enzymes that catalyze the oxidation

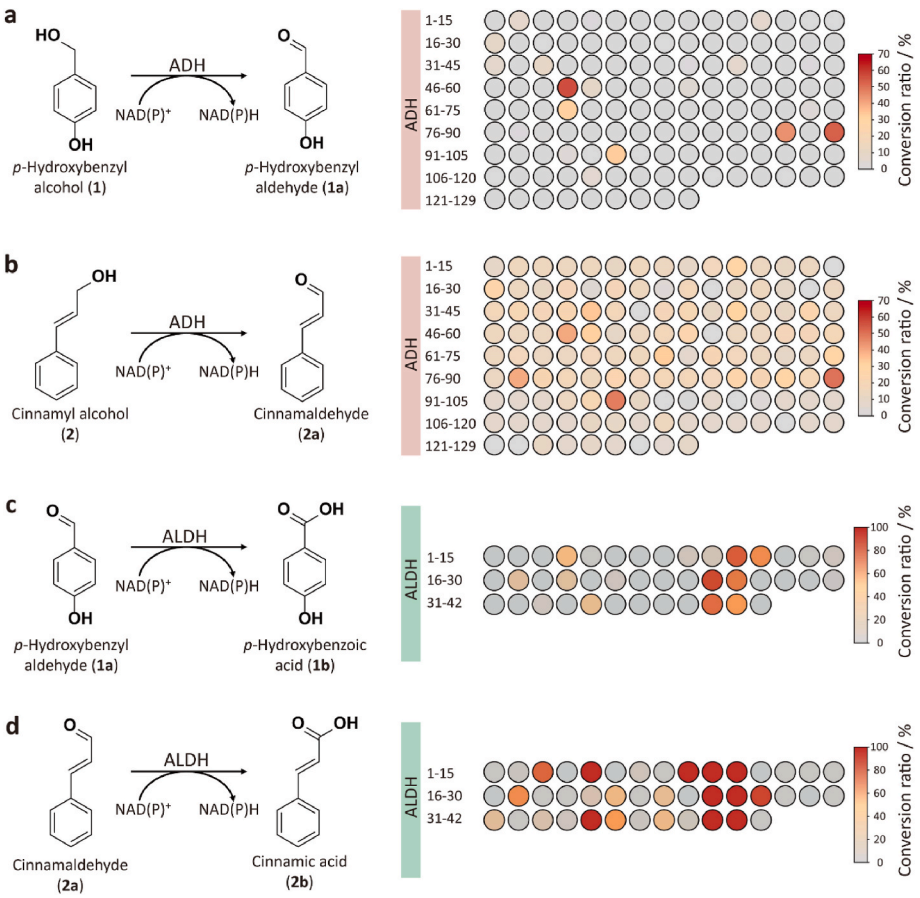

Fig. 2. Activity screening of ADHs and ALDHs. (a) *p*-hydroxybenzyl alcohol, (b) cinnamyl alcohol, (c) *p*-hydroxybenzyl aldehyde, and (d) cinnamaldehyde were used as substrates.

of hydroxyl groups to carbonyl groups or further to carboxyl groups. Some of these dehydrogenases, such as ADH CreG (for oxidation of benzyl alcohols) and ALDH CreC (for oxidation of benzyl aldehyde) from *C. glutamicum* [36], and ADH AdhA (for biotransformation a wide variety of aromatic alcohols) from *R. opacus* [37], have been studied for their roles and mechanisms in the metabolism of phenolic compounds. These enzyme resources in the genomic data of environmental microorganisms provide a material basis for mining efficient dehydrogenases.

The ADHs include two main families differing in their structural features: the "short-chain" enzymes have a single domain of enoyl-(acyl carrier protein) reductase, adh_short_C2 (PF13561), while the "medium-chain" zinc enzymes have two domains, namely a GroES-like alcohol dehydrogenase domain, ADH_N (PF08240), and a zinc-binding dehydrogenase domain, ADH_zinc_N (PF00107) [38]. On the other hand, the ALDHs share one common domain of aldehyde dehydrogenase family, Aldedh (PF00171), which is responsible for the oxidation of aldehydes to carboxylic acids [18]. To identify ADH genes in the genomes of *P. aeruginosa* PAO1, *C. glutamicum* ATCC 13032, and *B. subtilis* subsp. 168, we conducted Hidden Markov Model (HMM) searches using the ADH Pfam models of adh_short_C2 (PF13561), ADH_N (PF08240), and ADH_zinc_N (PF00107) as queries. This resulted in a total of 129 candidate ADHs (Tables S3 and S4), comprising 89 "short-chain" type and 40 "medium-chain" type enzymes (Fig. 1). Similarly, we identified 42 candidate ALDHs by querying the genomes with the ALDH Pfam model of Aldedh (PF00171) (Fig. 1, Table S5). Then, all candidate ADHs and ALDHs were amplified from the genomes, cloned into pET30a and transformed into *E. coli* BL21(DE3) to obtain heterologous expression strains (namely BADH1-BADH129 and BALDH1-BALDH42, respectively; Table S1).

3.2. Activity screening of alcohol dehydrogenases and aldehyde dehydrogenases

Single clones of strains BADH1-BADH129 and BALDH1-BALDH42 were picked and cultured overnight to make seed liquid, which was then inoculated into TB medium. The strains were grown in shake flasks at 37 °C until the mid-logarithmic growth phase, and the enzyme expression was induced at 18 °C for 24 h. Cells were then harvested, and the crude enzyme solutions were obtained by cell lysis and used for the screening assays. *p*-Hydroxybenzyl alcohol and cinnamyl alcohol were chosen as representative substrates of benzyl alcohols and phenylpropanoid alcohols for the activity screening of ADHs, respectively. Among the tested ADH enzymes, ADH-49, ADH-64, ADH-88, ADH-90, and ADH-96 showed high activity in oxidizing *p*-hydroxybenzyl alcohol to *p*-hydroxybenzaldehyde, with over 30% conversion rate (Fig. 2a). Moreover, ADH-49, ADH-88, ADH-90, and ADH-96 also exhibited remarkable activity in oxidizing cinnamyl alcohol to cinnamaldehyde (Fig. 2b). Consequently, these 4 ADHs were selected as potential candidates for further characterization. Similarly, *p*-hydroxybenzaldehyde and cinnamaldehyde were used as test substrates for ALDHs, resulting in the identification of four potential ALDHs (ALDH-11, ALDH-25, ALDH-26, and ALDH-40) with significant catalytic activity among 42 ALDH candidates. The four ALDHs were able to oxidize *p*-hydroxybenzaldehyde and cinnamaldehyde into corresponding acid products with >70% and 100% conversion ratios, respectively (Fig. 2c and d). We then investigated the cofactor preferences of the top enzymes ADH-49, ADH-88, ADH-90, ADH-96, ALDH-11, ALDH-25, ALDH-26 and ALDH-40 using either $NADP^+$ or NAD^+. ADH-88, ADH-90 and the four ALDH could use either $NADP^+$ or NAD^+ (Fig. S6). Both ADH-49 and ADH-96 could only use NAD^+ as cofactor. ALDH-11, ALDH-26, ALDH-40 and

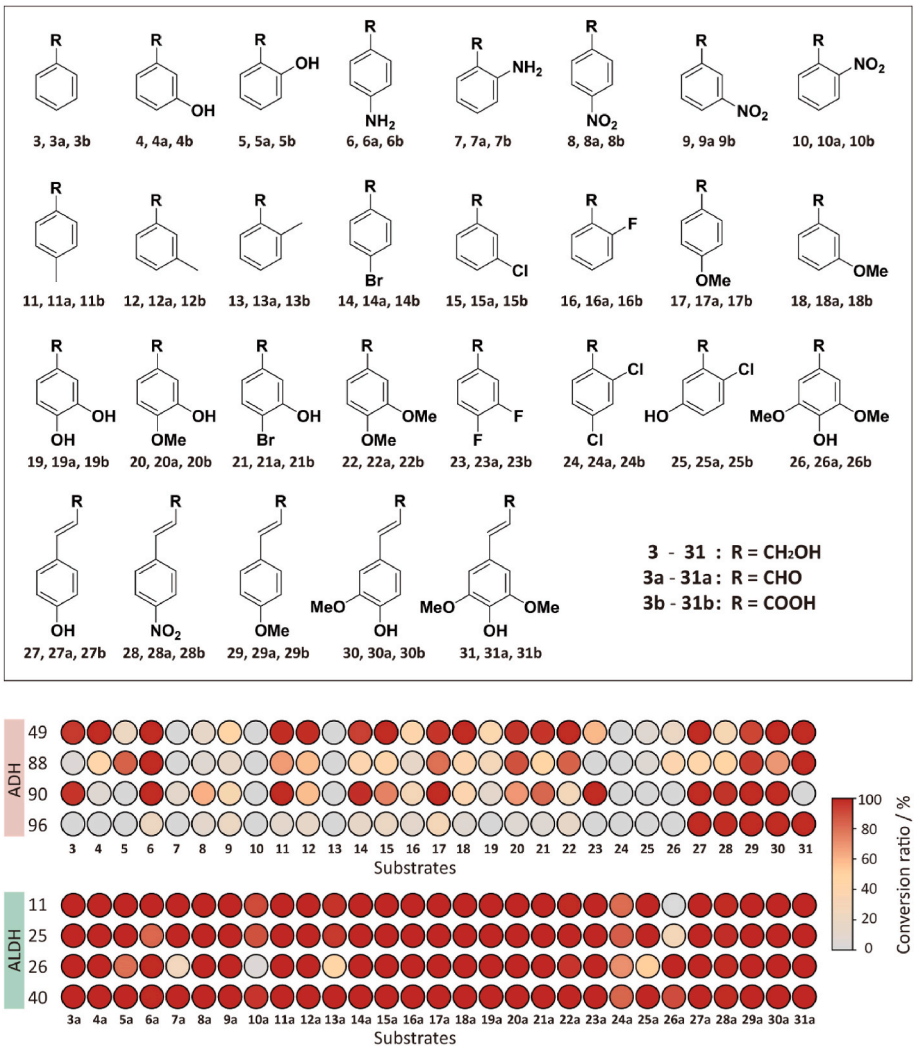

Fig. 3. Exploration of the substrate promiscuity of potential ADHs and ALDHs. Upper panel, structures of substrates and products. Lower panel, conversion rates.

ADH-90 showed a strong preference for NAD^+ over $NADP^+$, while ADH-88 exhibited increased activity with $NADP^+$ compared to NAD^+. These results demonstrate the feasibility of screening and identifying novel ADHs and ALDHs from genomic library of environmental microorganisms for the biosynthesis of benzyl and phenylpropanoid compounds.

3.3. Exploration of the substrate promiscuity of alcohol dehydrogenases and aldehyde dehydrogenases

To fully exploit the potential of dehydrogenases for the biosynthesis of aromatic compounds, the substrate promiscuity of the selected ADHs and ALDHs was investigated in detail. A major challenge for the application of dehydrogenases is the requirement of costly cofactors (NAD(P)$^+$) as co-substrates for their catalytic activity [39]. To overcome this limitation, a NAD(P)H oxidase (LreNox) [40] from *L. reuteri* was co-expressed with the dehydrogenases to achieve cofactor recycling. The activity and kinetic parameters of NOX had been determined using NADH or NADPH in previous report, showing that LreNox exhibits high efficiency for oxidizing both NADH and NADPH. The kinetic parameters for LreNox were determined under increasing concentrations of NADH and NADPH, revealing that the K_m and K_{cat} values for both NADH and NADPH were similar [40]. The effect of LreNox on the conversion rate of *m*-hydroxybenzyl alcohol (**4**) to *m*-hydroxybenzaldehyde (**4a**) by ADH-49 was tested as an example. The results showed that co-expression of LreNox with ADH-49 increased the conversion rate by as high as 7.2-fold within 270 min of reaction (Fig. S1), demonstrating the effectiveness of this strategy. Following above activity screening, the 4 ADH and 4 ALDH candidate enzymes were purified (Fig. S2), and the substrate promiscuity was further evaluated under the LreNox-mediated cofactor recycling conditions. Twenty-four types of benzyl alcohols and five types of phenylpropanoid alcohols were used as substrates to test the 4 ADHs (ADH-49, ADH-88, ADH-90, and ADH-96). The reaction mixtures containing 10 μM ADH and 10 μM LreNox were incubated at 30 °C for 3 h, and the conversion rates were measured.

ADH-49 demonstrated remarkable efficiency and selectivity in oxidizing most of the *meta*- or *para*-substituted benzyl alcohols, achieving over 90% conversion of *m*-hydroxybenzyl alcohol (**4**), *p*-aminobenzyl alcohol (**6**), *p*-methylbenzyl alcohol (**11**), *m*-methylbenzyl alcohol (**12**), *p*-bromobenzyl alcohol (**14**), *m*-chlorobenzyl alcohol (**15**), *p*-methylbenzyl alcohol (**17**), and *m*-methylbenzyl alcohol (**18**) into the corresponding aldehydes (Fig. 3), while exhibited poor or no oxidation for *ortho*-substituted benzyl alcohol substrates (**5**, **7**, **10**, **13**, and **16**). Interestingly, the oxidation of *p*-nitrobenzyl alcohol (**8**) and *m*-nitrobenzyl alcohol (**9**) was relatively low, with no more than 50% conversion observed. Meanwhile, ADH-49 was able to oxidize over 90% of phenylpropanoid alcohols (**27**, **29**, **30**, and **31**) without nitro substituents into corresponding phenylpropanoid aldehydes. ADH-88 exhibited efficient oxidation of some benzyl alcohols (**5**, **6**, **11**, **17**, **20**, and **22**) and phenylpropanoid alcohols (**29**, **30**, and **31**) with more than 60% conversion, but it showed a narrower substrate range than ADH-49.

Furthermore, when both ADH-49 and ADH-88 could catalyze the same benzyl alcohols (**6**, **11**, **17**, **20**, and **22**), ADH-49 showed higher catalytic efficiency than ADH-88.

ADH-90 exhibited excellent oxidation of *para*-monosubstituted benzyl alcohols (**6**, **8**, **11**, **14**, and **17**), but had limited activity for other mono-substituted ones (**4**, **5**, **7**, **9**, **10**, **12**, **13**, **16**, and **18**), as well as some di- or multi-substituted benzyl alcohol substrates (**19**, **22**, **24**, **25**, and **26**). Intriguingly, ADH-90 showed good catalytic activity (with the conversion ratio of 100%) for *p*,*m*-difluorobenzyl alcohol **23**, likely due to the minimal steric hindrance of the fluorine atoms. Furthermore, compared with the low conversion ratio (15.4%) of ADH-49, ADH-90 converted 61.5% of *p*-nitrobenzyl alcohol (**8**) into *p*-nitrobenzaldehyde (**8a**). The above results showed that although different from ADH-49 in having broader substrate specificity, ADH-90 is more efficient at catalyzing *para* substituted substrates. Additionally, ADH-90 oxidized the most tested phenylpropanoid alcohols (except for **31**) into aldehydes completely, indicating its advantage in oxidizing small hindered phenylpropanoid alcohols, consistent with its oxidation pattern for benzyl alcohols. Moreover, ADH-96 exhibited limited catalytic activity on benzyl alcohols but demonstrated excellent preference for all tested phenylpropanoid alcohols.

Following the same approach as for the alcohol dehydrogenases, the substrate promiscuity of the 4 ALDHs (ALDH-11, ALDH-25, ALDH-26, and ALDH-40) was assessed using 24 benzyl aldehydes and 5 phenylpropanoid aldehydes. The 4 ALDHs completely oxidized almost all of the tested aldehydes. ALDH-40 showed oxidation activity for all tested substrates except **24a** (conversion ratio, 84%), with remarkable conversion rates above 90% for the remaining substrates. On the other hand, the catalytic efficiencies of ALDH-11 and ALDH-25 for the tested tri-substituted benzyl aldehyde (**26a**) were considerably lower than that of ALDH-40. In addition, ALDH-26 exhibited a slightly lower oxidation efficacy (<50%) for *o*-aminobenzaldehyde (**7a**), *o*-nitrobenzaldehyde (**10a**), *o*-tolualdehyde (**13a**), and other *ortho*-monosubstituted benzyl aldehydes, and its catalytic efficiency for **25a** was also inferior to the other three ALDHs.

Taken together, the results indicated that the four ADHs and ALDHs had different substrate preferences and catalytic efficiencies for benzyl alcohols and phenylpropanoid alcohols. ADH-49 was effective for *meta-*/*para*-substituted benzyl alcohols and phenylpropanoid alcohols without nitro substituents, but less so than ADH-90 for the *para*-substituted benzyl alcohols and ADH-96/ADH-90 for the phenylpropanoid alcohols. Therefore, ADH-49 was suitable for *meta*-substituted benzyl alcohol and *para*- and *meta*-disubstituted benzyl alcohol, while ADH-90 was the best enzyme for *para*-substituted benzyl alcohols. Both ADH-90 and ADH-96 showed high catalytic efficiency for phenylpropanoid alcohols with small steric hindrance, while ADH-96 was the most efficient enzyme for phenylpropanoids with large steric hindrance. In contrast, ADH-88 had a narrow substrate range and low catalytic efficiency, making it an unlikely choice as the preferred candidate ADH under normal conditions. Among the 4 ALDHs, ALDH-40 exhibited superior ability for oxidizing benzyl and phenylpropanoid aldehydes, surpassing the other three enzymes and thus being the most preferred ALDH.

In addition, previous studies have shown that ADHs and ALDHs employ different catalytic mechanisms in the alcohol and aldehyde oxidation processes \[18,41]. The “short-chain” type of ADHs uses a universal base (B) as the acceptor of the hydroxyl proton, and the alcohol substrate is oxidized to the aldehyde by hydride transfer (Fig. S3a) [42]. The “medium-chain” type of ADHs interact with the coenzyme $NAD(P)^+$ and coordinate with zinc(II) ions to bind alcohol substrates. Through a series of deprotonation steps, the hydrides are transferred from the alkoxide ions to $NAD(P)^+$ to form zinc-bound aldehydes or ketones and NAD(P)H, and then the aldehydes are then released (Fig. S3b) [19]. ALDHs also depend on the cofactor $NAD(P)^+$. Aldehydes enter the enzyme’s active pocket through surface channels. The sulfur group of the active cysteine residue undergoes nucleophilic attack on the aldehydes’ carbonyl carbon and the hydrides then attack $NAD(P)^+$ to generate NAD(P)H. Subsequently, a conformational change occurs in the active pocket, leading to NAD(P)H displacement and water molecule entry. Under the mediation of the active glutamate residue, the water molecule attacks the carbonyl carbon, resulting in the formation of carboxylic acid (Fig. S4) [18]. Interestingly, in this study, some of the identified alcohol dehydrogenases (ADH-49, ADH-88 and ADH-90) have been found to have the ability to continuously oxidize alcohol substrates into carboxylic acids (Fig. S5). The enzymes’ dual functionality disrupts the isolation between alcohol dehydrogenases and aldehyde dehydrogenases. It can be speculated that these enzymes may have evolved different catalytic mechanisms to achieve the oxidation of both alcohols and aldehydes. A thorough understanding of the mechanism underlying these bifunctional enzymes can help future efforts to rationally engineer ADHs and ALDHs and identify more potential dehydrogenases.

3.4. Scaled-up production of benzyl and phenylpropanoid acids via a whole-cell catalytic system

Many benzyl and phenylpropanoid alcohols are environmental hazards due to their cytotoxicity [43]. Nevertheless, these compounds can be transformed into synthetic drug intermediates or products by oxidizing them to carboxylic acid derivatives [44]. Hence, we aimed to develop an enzymatic cascade whole-cell system, employing dehydrogenase oxidation and cofactor regeneration processes to convert benzyl and phenylpropanoid alcohols directly into carboxylic acids.

Cinnamic acid (**2b**), renowned for its honey-like aroma, plays a pivotal role in the synthesis of methyl cinnamate, ethyl cinnamate, and benzyl cinnamate in the perfume industry [45]. Furthermore, it serves as a key intermediate in the biosynthesis of various natural compounds such as lignin, flavonoids, isoflavones, coumarin, aurone, stilbenes, catechins, and phenylpropenes [46]. Additionally, **2b** acts as a precursor for the sweetener aspartame [47]. Likewise, *p*-toluic acid (**11b**) has a crucial role as an intermediate in polymer stabilizers, photosensitizing compounds, animal feed supplements, and other organic chemicals including pharmaceuticals, pigments, and dyes [48]. The production of **2b** and **11b** has significant medical and economic value. In view of the aforementioned applications, we aimed to establish a comprehensive whole-cell catalytic system for the conversion of **2** and **11** into **2b** and **11b**, respectively. For substrate **2**, belonging to *para*-substituted benzyl alcohols, ADH-90 emerges as the optimal choice ($K_m = 1.7 \pm 0.3$ mM, $k_{cat} = 14.3 \pm 1.2$ min^{-1}, Fig. S8a). Substrate **11**, a phenylpropanoid alcohol with limited steric hindrance, suggests the potential use of ADH-90 and ADH-96 as preferred ADHs. Meanwhile, ALDH-40 exhibits the broadest substrate range and promising catalytic activity for aldehyde substrates, making it the most suitable ALDH (The K_m and k_{cat} values towards **2a** were 10.0 ± 2.7 mM and $(3.3 \pm 0.7) \times 10^2$ min^{-1}, and the K_m and k_{cat} values towards **11a** were 10.0 ± 4.1 mM and $(1.8 \pm 0.6) \times 10^2$ min^{-1}. Figs. S8c and d). Taking these factors into account, we selected ADH-90 and ALDH-40 as biocatalysis enzymes, together with the NAD(P)H oxidase LreNox to construct the whole-cell catalytic system. The K_m and k_{cat} values of ADH-90 towards **11** were 1.2 ± 0.1 mM and 6.7 ± 0.3 min^{-1} (Fig. S8b).

The effect of thermal stability on ADH-90 and ALDH-40 were monitored at seven temperatures of 0, 25, 30, 35, 40, 45, and 50 °C for 30 min. Reactions were carried out in triplicates with 1 mM substrate, 0.5 μM ADH-90 or ALDH-40, and 2 mM NADP+. For ADH-90, the maximum conversion of substrate **2** (8.0%) was achieved at temperatures of 40 °C and 45 °C (Fig. S7a). The conversion rate variance between 30 and 40/45 °C is relatively small, with a difference of less than 1.5%. The maximum conversion of substrate **2a** by ALDH-40 was attained at 30 °C, resulting in a yield of 61.0 % (Fig. S7b). A decrease in yield was observed at elevated temperatures of 35 °C, 40 °C, 45 °C, and 50 °C. Compared to ALDH-40, ADH-90 has better thermal stability. Among the temperatures tested, 30 °C and 40 °C demonstrated enhanced catalytic efficiency for both ADH-90 and ALDH-40. While 40 °C resulted in a relatively higher conversion rate for ADH-90, it was

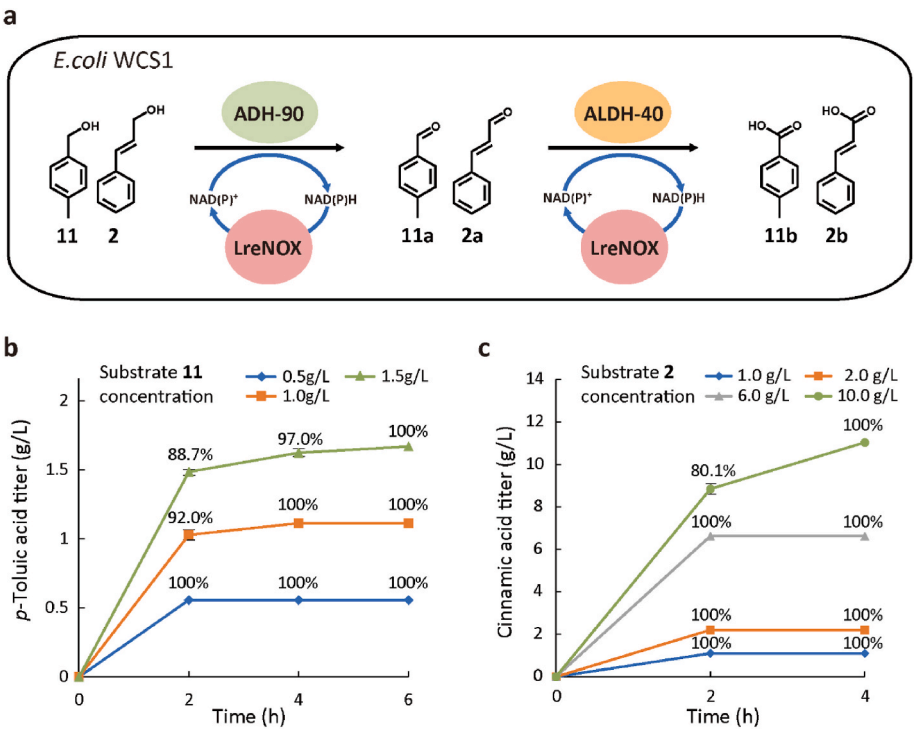

Fig. 4. Whole-cell cascade catalytic system for production of benzyl and phenylpropanoid acids. (a) The whole-cell catalysis scheme. (b) Whole-cell transformation of **11**. (c) Whole-cell transformation of **2**.

noted that this temperature would dramatically decrease the activity of ALDH-40 by 16 %. Therefore, 30 °C was selected as the optimal temperature for driving the cascade biocatalysis.

To obtain the whole-cell transformant WCS1 (Fig. 4a), we co-transformed *E. coli* BL21(DE3) cells with two plasmids: one expressing the LreNox gene (pET28a-LreNOX) and another expressing both the ADH-90 and ALDH-40 genes (pETDuet-1-ADH-90-2-ALDH-40). After enzyme expression, the bacterial cells were collected and resuspended in a solution of OD_{600} = 27 for following whole-cell catalysis. We tested different concentrations of **11** (0.5 g/L, 1.0 g/L, and 1.5 g/L) as substrates and collected samples at 2 h, 4 h, and 6 h of reaction to evaluate the production of **11b** (Fig. 4b). Within 2 h of the whole-cell catalytic reaction, substrate **11** at concentrations of 0.5, 1.0 and 1.5 g/L were converted into **11b** with conversion efficiencies of 100%, 92.0%, and 88.7%, respectively. After 4 h of reaction, complete oxidation of 1.0 g/L substrate was achieved, while 97.0% of 1.5 g/L substrate was oxidized. For 6 h of reaction, 1.5 g/L of **11** was fully converted into product.

Likewise, we used various concentrations of **2** (1 g/L, 2 g/L, 6 g/L, and 10 g/L) as substrates and took samples were taken at 2 h and 4 h of reaction to measure production (Fig. 4c). After 2 h of reaction, the whole-cell system completely oxidized 1 g/L, 2 g/L, and 6 g/L of substrate **2** into product **2b**. For 10 g/L of the substrate, 8.85 g/L of the product was produced, corresponding to a conversion rate of 80.1%. After 4 h of reaction, complete oxidation of 10 g/L substrate was achieved, indicating the high efficiency of the whole-cell system for phenylpropanoid alcohol conversion.

These results demonstrate that the whole-cell cascade catalytic system developed can effectively biocatalyze **11** and **2** into corresponding carboxylic acids, which can be easily scaled up to gram level, providing a method for the preparation of pharmaceutical intermediates and products. It is anticipated that, by adjusting the candidate enzymes according to the substrate, the whole-cell system can be easily extended to the production of other benzyl and phenylpropanoid alcohols, offering substantial economic and production benefits.

4. Conclusions

Multiple ADHs and ALDHs were identified and characterized from genomic data of environmental microorganisms that can oxidize benzyl/phenylpropanoid alcohols and aldehydes. The optimal ADH-90 and ALDH-40 with higher catalytic activity and broader substrate preferences were selected, together with the NAD(P)H oxidase LreNox, to construct a whole-cell cascade catalytic system. This system can oxidize many benzyl alcohols and phenylpropanoid alcohols in a green and efficient manner. It effectively transformed gram-scale quantities of *p*-methylbenzyl alcohol and cinnamyl alcohol to the respective carboxylic acids. The mining-test-analyze-build strategy of this study also provides new insights for realizing the green biosynthesis of other valuable aromatic products.

CRediT authorship contribution statement

Zetian Qiu: performed the experiment and prepared original draft. **Xiaohui Liu and Yushuo Zhao:** performed the experiment. **Jie Yu and Kun Liu:** analyzed the data. **Guang-Rong Zhao:** prepared the manuscript. **Shengying Li:** prepared the manuscript. **Lei Du:** conceived, and designed the experiment, prepared the manuscript. **Li Ma:** cconceived, and designed the experiment, prepared the manuscript. All authors read and approved the final manuscript.

Declaration of competing interest

The authors declare that they have no known competing financial interests or personal relationships that could have appeared to influence the work reported in this paper.

Acknowledgments

This work was supported by the National Key Research and Development Program of China (2021YFA0911500), the National Natural Science Foundation of China (32071266, 32170088, and 32370032),

the Shandong Provincial Natural Science Foundation (ZR2020ZD23), and the State Key Laboratory of Microbial Technology Open Projects Fund (M2022-01).

Appendix B. Supplementary data

Supplementary data to this article can be found online at https://doi.org/10.1016/j.synbio.2024.01.008.

References

[1] Shen YP, Niu FX, Yan ZB, Fong LS, Huang YB, Liu JZ. Recent advances in metabolically engineered microorganisms for the production of aromatic chemicals derived from aromatic amino acids. Front Bioeng Biotechnol 2020;8:407. https://doi.org/10.3389/fbioe.2020.00407.

[2] Dickey RM, Forti AM, Kunjapur AM. Advances in engineering microbial biosynthesis of aromatic compounds and related compounds. Bioresour. Bioprocess 2021;8(1):1–17. https://doi.org/10.1186/s40643-021-00434-x.

[3] Huang XQ, Li RQ, Fu JX, Dudareva N. A peroxisomal heterodimeric enzyme is involved in benzaldehyde synthesis in plants. Nat Commun 2022;13(1):1352. https://doi.org/10.1038/s41467-022-28978-2.

[4] Valanciene E, Jonuskiene I, Syrpas M, Augustiniene E, Matulis P, Simonavicius A, Malys N. Advances and prospects of phenolic acids production, biorefinery and analysis. Biomolecules 2020;10(6):874. https://doi.org/10.3390/biom10060874.

[5] Cao MF, Gao MR, Suastegui M, Mei YZ, Shao ZY. Building microbial factories for the production of aromatic amino acid pathway derivatives: from commodity chemicals to plant-sourced natural products. Metab Eng 2020;58:94–132. https://doi.org/10.1016/j.ymben.2019.08.008.

[6] Sajid M, Channakesavula CN, Stone SR, Kaur P. Synthetic biology towards improved flavonoid pharmacokinetics. Biomolecules 2021;11(5):754. https://doi.org/10.3390/biom11050754.

[7] Yuan SF, Yi X, Johnston TG, Alper HS. De novo resveratrol production through modular engineering of an *Escherichia coli-Saccharomyces cerevisiae* co-culture. Microb Cell Factories 2020;19(1):1–12. https://doi.org/10.1186/s12934-020-01401-5.

[8] Ahmad JU, Raisanen MT, Leskela M, Repo T. Copper catalyzed oxidation of benzylic alcohols in water with H_2O_2. Appl Catal Gen 2012;411:180–7. https://doi.org/10.1016/j.apcata.2011.10.038.

[9] Das R, Chakraborty D. Cu(II) bromide catalyzed oxidation of aldehydes and alcohols. Appl Organomet Chem 2011;25(6):437–42. https://doi.org/10.1002/aoc.1783.

[10] Xu C, Zhang CH, Li H, Zhao XY, Song L, Li XB. An overview of selective oxidation of alcohols: catalysts, oxidants and reaction mechanisms. Catal Surv Asia 2016;20(1):13–22. https://doi.org/10.1007/s10563-015-9199-x.

[11] Davis SE, Ide MS, Davis RJ. Selective oxidation of alcohols and aldehydes over supported metal nanoparticles. Green Chem 2013;15(1):17–45. https://doi.org/10.1039/c2gc36441g.

[12] Chen J, Zhang Y, Zhu DJ, Li T. Selective oxidation of alcohols by porphyrin-based porous polymer-supported manganese heterogeneous catalysts. Appl Organomet Chem 2020;34(2):e5259. https://doi.org/10.1002/aoc.5259.

[13] Xie JH, Yin KH, Serov A, Artyushkova K, Pham HN, Sang XH, Unocic RR, Atanassov P, Datye AK, Davis RJ. Selective aerobic oxidation of alcohols over atomically-dispersed non-precious metal catalysts. ChemSusChem 2017;10(2):359–62. https://doi.org/10.1002/cssc.201601364.

[14] Heravi MM, Momeni T, Zadsirjan V, Mohammadi L. Applications of the dess-martin oxidation in total synthesis of natural products. Curr Org Synth 2021;18(2):125–96. https://doi.org/10.2174/1570179417666200917102634.

[15] Bleie O, Roberto MF, Dearing TI, Branham CW, Kvalheim OM, Marquardt BJ. Moffat-swern oxidation of alcohols: translating a batch reaction to a continuous-flow reaction. J. Flow Chem. 2015;5(3):183–9. https://doi.org/10.1556/1846.2015.00025.

[16] Torbina VV, Vodyankin AA, Ten S, Mamontov GV, Salaev MA, Sobolev VI, Vodyankina OV. Ag-based catalysts in heterogeneous selective oxidation of alcohols: a review. Catalysts 2018;8(10):447. https://doi.org/10.3390/catal8100447.

[17] Puetz H, Puch'ova E, Vrankova K, Hollmann F. Biocatalytic oxidation of alcohols. Catalysts 2020;10(9):952. https://doi.org/10.3390/catal10090952.

[18] Shortall K, Djeghader A, Magner E, Soulimane T. Insights into aldehyde dehydrogenase enzymes: a structural perspective. Front Mol Biosci 2021;8:659550. https://doi.org/10.3389/fmolb.2021.659550.

[19] An JH, Nie Y, Xu Y. Structural insights into alcohol dehydrogenases catalyzing asymmetric reductions. Crit Rev Biotechnol 2019;39(3):366–79. https://doi.org/10.1080/07388551.2019.1566205.

[20] Ho KL, Lin B, Chen YY, Lee DJ. Biodegradation of phenol using *Corynebacterium* sp DJ1 aerobic granules. Bioresour Technol 2009;100(21):5051–5. https://doi.org/10.1016/j.biortech.2009.05.050.

[21] Yotinov I, Todorova Y, Schneider I, Daskalova E, Topalova Y. The effect of nanodiamonds on phenol biodegradation by *Pseudomonas* sp. strain isolated from polluted sediments. J Neurol Neurophysiol 2016;16(7):7696–706. https://doi.org/10.1166/jnn.2016.11295.

[22] Diksha, Kumar R, Kumar S, Kumari A, Panwar A. Biodegradation of phenol-rich sewage water using indigenous bacterial consortium: a laboratory- to plant-scale study. Int J Environ Sci Technol 2023;14:1–16. https://doi.org/10.1007/s13762-023-04892-y.

[23] Ziagova MG, Liakopoulou-Kyriakides M. Comparative studies on the degradation of three aromatic compounds by Pseudomonas sp and Staphylococcus xylosus. J. Environ. Sci. Health, Pt. A: Environ. Sci. Eng. Toxic Hazard. Subst. Control 2010;45(8):1017–25. https://doi.org/10.1080/10934521003772444.

[24] Wang YH, Huang Z, Liu SJ. Chemotaxis towards aromatic compounds: insights from comamonas testosteroni. Int J Mol Sci 2019;20(11):2701. https://doi.org/10.3390/ijms20112701.

[25] Kivisaar M. Degradation of nitroaromatic compounds: a model to study evolution of metabolic pathways. Mol Microbiol 2009;74(4):777–81. https://doi.org/10.1111/j.1365-2958.2009.06905.x.

[26] Diaz E, Jimenez JI, Nogales J. Aerobic degradation of aromatic compounds. Curr Opin Biotechnol 2013;24(3):431–42. https://doi.org/10.1016/j.copbio.2012.10.010.

[27] Zhong QZ, Zhang HY, Bai WQ, Li M, Li BT, Qiu XH. Degradation of aromatic compounds and degradative pathway of 4-nitrocatechol by Ochrobactrum sp B2. J. Environ. Sci. Health, Pt. A: Environ. Sci. Eng. Toxic Hazard. Subst. Control 2007;42(14):2111–6. https://doi.org/10.1080/10934520701627108.

[28] Du L, Ma L, Qi FF, Zheng XL, Jiang CY, Li AL, Wan XB, Liu SJ, Li SY. Characterization of a unique pathway for 4-cresol catabolism initiated by phosphorylation in *Corynebacterium glutamicum*. J Biol Chem 2016;291(12):6583–94. https://doi.org/10.1074/jbc.M115.695320.

[29] Qin W, Liu G. Microbial Technology for biosustainability. Eng. Microbiol. 2023;3(2):100088. https://doi.org/10.1016/j.engmic.2023.100088.

[30] Falkowski PG, Fenchel T, Delong EF. The microbial engines that drive earth's biogeochemical cycles. Science 2008;320(5879):1034–9. https://doi.org/10.1126/science.1153213.

[31] De Lorenzo V. Systems biology approaches to bioremediation. Curr Opin Biotechnol 2008;19(6):579–89. https://doi.org/10.1016/j.copbio.2008.10.004.

[32] Ahmed AM, Nakhla GF, Farooq S. Phenol degradation by Pseudomonas aeruginosa. J. Environ. Sci. Health, Pt. A: Environ. Sci. Eng. Toxic Hazard. Subst. Control 1995;30(1):99–107. https://doi.org/10.1080/10934529509376188.

[33] Aravindhan R, Naveen N, Anand G, Rao JR, Nair BU. Kinetics of biodegradation of phenol and a polyphenolic compound by a mixed culture containing *Pseudomonas aeruginosa* and *Bacillus subtilis*. Appl Ecol Environ Res 2014;12(3):615–25. https://doi.org/10.15666/aeer/1203_615625.

[34] Ezhilkumar P, Sivakumar VM, Yogasri A, Thirumarimurugan M. Biodegradation of formaldehyde using *Bacillus subtilis* in batch process. Int J Mater Prod Technol 2017;55(1–3):296–307. https://doi.org/10.1504/Ijmpt.2017.084963.

[35] Zheng YL, Liu DL, Liu SW, Xu SY, Yuan YZ, Xiong L. Kinetics and mechanisms of *p*-nitrophenol biodegradation by *Pseudomonas aeruginosa* HS-D38. J Environ Sci (China) 2009;21(9):1194–9. https://doi.org/10.1016/S1001-0742(08)62403-1.

[36] Du L, Dong S, Zhang XW, Jiang CY, Chen JF, Yao LS, Wang X, Wan XB, Liu X, Wang XQ, Huang SH, Cui Q, Feng YG, Liu SJ, Li SY. Selective oxidation of aliphatic C-H bonds in alkylphenols by a chemomimetic biocatalytic system. Proc Natl Acad Sci USA 2017;114(26):E5129–37. https://doi.org/10.1073/pnas.1702317114.

[37] Xue P, Taki H, Komukai S, Sekine M, Kanoh K, Kasai H, Choi SK, Omata S, Tanikawa S, Harayama S, Misawa N. Characterization of four *Rhodococcus* alcohol dehydrogenase genes responsible for the oxidation of aromatic alcohols. Appl Microbiol Biotechnol 2006;71(6):824–32. https://doi.org/10.1007/s00253-005-0204-6.

[38] Danielsson O, Atrian S, Luque T, Hjelmqvist L, Gonzalezduarte R, Jornvall H. Fundamental molecular differences between alcohol-dehydrogenase classes. Proc Natl Acad Sci USA 1994;91(11):4980–4. https://doi.org/10.1073/pnas.91.11.4980.

[39] Xie S, Zhang L. A specialized role played by a redox cofactor. Eng. Microbiol. 2022;2(1):100010. https://doi.org/10.1016/j.engmic.2022.100010.

[40] Gao H, Li J, Sivakumar D, Kim TS, Patel SKS, Kalia VC, Kim IW, Zhang YW, Lee JK. NADH oxidase from *Lactobacillus reuteri*: a versatile enzyme for oxidized cofactor regeneration. Int J Biol Macromol 2019;123:629–36. https://doi.org/10.1016/j.ijbiomac.2018.11.096.

[41] De Miranda AS, Milagre CDF, Hollmann F. Alcohol dehydrogenases as catalysts in organic synthesis. Front. Catal. 2022;2:900554. https://doi.org/10.3389/fctls.2022.900554.

[42] Chen J, Yu Y, Gao JJ, Yang SL. UDP-glucose dehydrogenase: the first-step oxidation is an $NAD(^+)$-dependent bimolecular nucleophilic substitution reaction (S_N2). Int J Biol Sci 2019;15(2):341–50. https://doi.org/10.7150/ijbs.28904.

[43] Sleat R, Robinson JP. The bacteriology of anaerobic degradation of aromatic-compounds. J Appl Bacteriol 1984;57(3):381–94. https://doi.org/10.1111/j.1365-2672.1984.tb01404.x.

[44] Bialecka-Florjanczyk E, Fabiszewska A, Zieniuk B. Phenolic acids derivatives - biotechnological methods of synthesis and bioactivity. Curr Pharmaceut Biotechnol 2018;19(14):1098–113. https://doi.org/10.2174/1389201020666181217142051.

[45] Yilmaz S, Sova M, Ergun S. Antimicrobial activity of trans-cinnamic acid and commonly used antibiotics against important fish pathogens and nonpathogenic isolates. J Appl Microbiol 2018;125(6):1714–27. https://doi.org/10.1111/jam.14097.

[46] Ruwizhi N, Aderibigbe BA. Cinnamic acid derivatives and their biological efficacy. Int J Mol Sci 2020;21(16):5712. https://doi.org/10.3390/ijms21165712.

[47] Patel AT, Akhani RC, Patel MJ, Dedania SR, Patel DH. Bioproduction of L-aspartic acid and cinnamic acid by L-aspartate ammonia lyase from *Pseudomonas aeruginosa* PAO1. Appl Biochem Biotechnol 2017;182(2):792–803. https://doi.org/10.1007/s12010-016-2362-7.

[48] Li HB, Hao MA, Qin C, Yang WB, Hu XP, Qin SY. An efficient aerobic oxidation for *p*-xylene to *p*-toluic acid catalyzed by cobalt (II) hydroxamates with benzo-15-

crown-5. React Kinet Catal Lett 2007;91(2):299–306. https://doi.org/10.1007/s11144-007-5144-y.